Jet Propulsion Laboratory
California Institute of Technology

First UAVSAR Deployment Results from a Polarimetric Active Radar Calibrator

Ronald J. Muellerschoen, Duan Xueyang, Jack Bush
Radar Science and Engineering
Jet Propulsion Laboratory, California Institute of Technology

Mani Kashanianfard, Adib Nashashibi, Kamal Sarabandi
Department of Electrical Engineering and Computer Science, University of Michigan

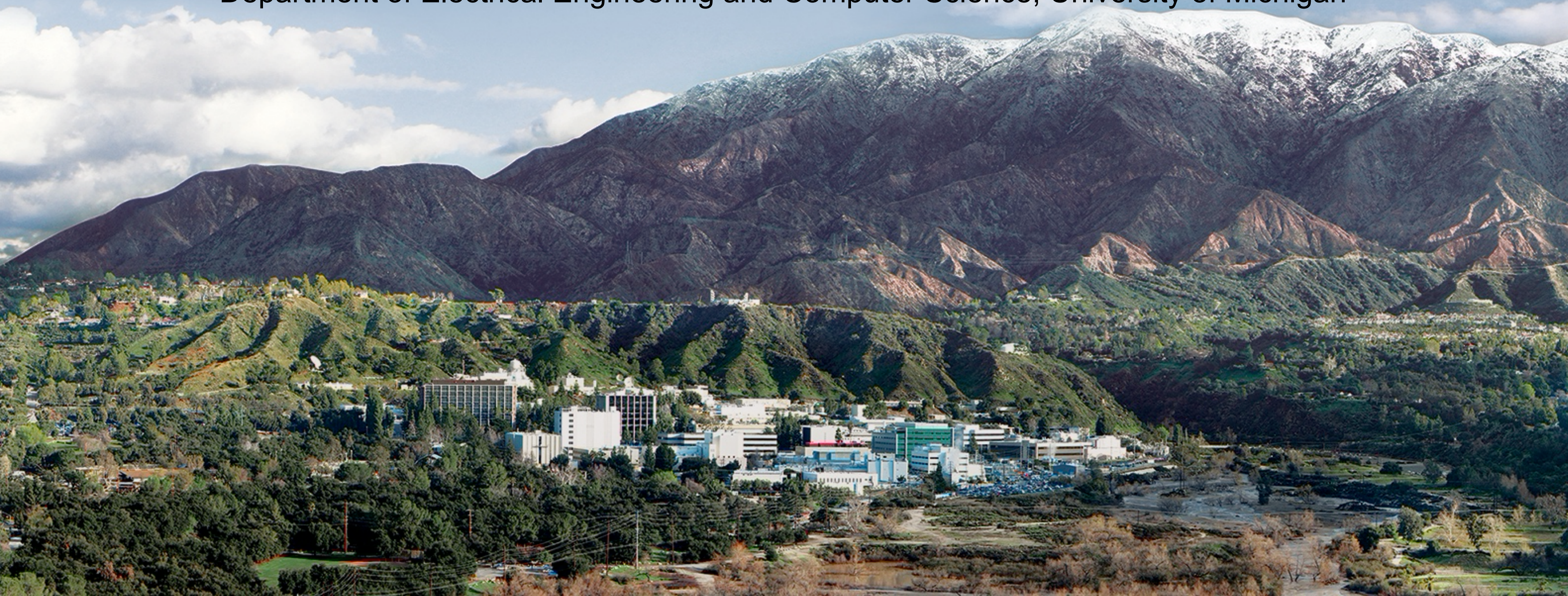

UAVSAR Airborne Instrument

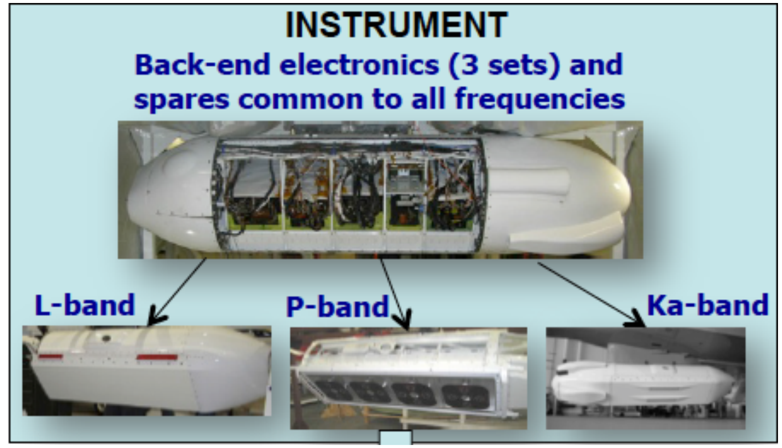

	P-band/UHF	L-band	Ka-band
Frequency (MHz)	280 – 440	1217.5-1297.5	35,620-35,700
Nominal Bandwidth (MHz)	20	80	80
Selectable Bandwidths (MHz)	6, 20, 40, 80	80	80
Polarization	Quad-pol	Quad-pol	Horizontal
Peak Transmit Power (kW)	2.0	3.1	0.08
Maximum Duty Cycle	10%	8%	10%
Look Angle Range	25 – 50 deg	25-65 deg	15-50
Nominal Range Swath (km)	9	22	10
Noise Equivalent Sigma0 (dB)	< -40	< -50	TBD
Radiometric Accuracy (dB)	< 1 absolute	< 1 absolute	TBD
Height Precision (30x30 m posting)	N/A	N/A	0.1 – 0.5 m

Rosamond Corner Reflector Array

UAVSAR 80 MHz Polarmetric L-band Image Sept, 2017

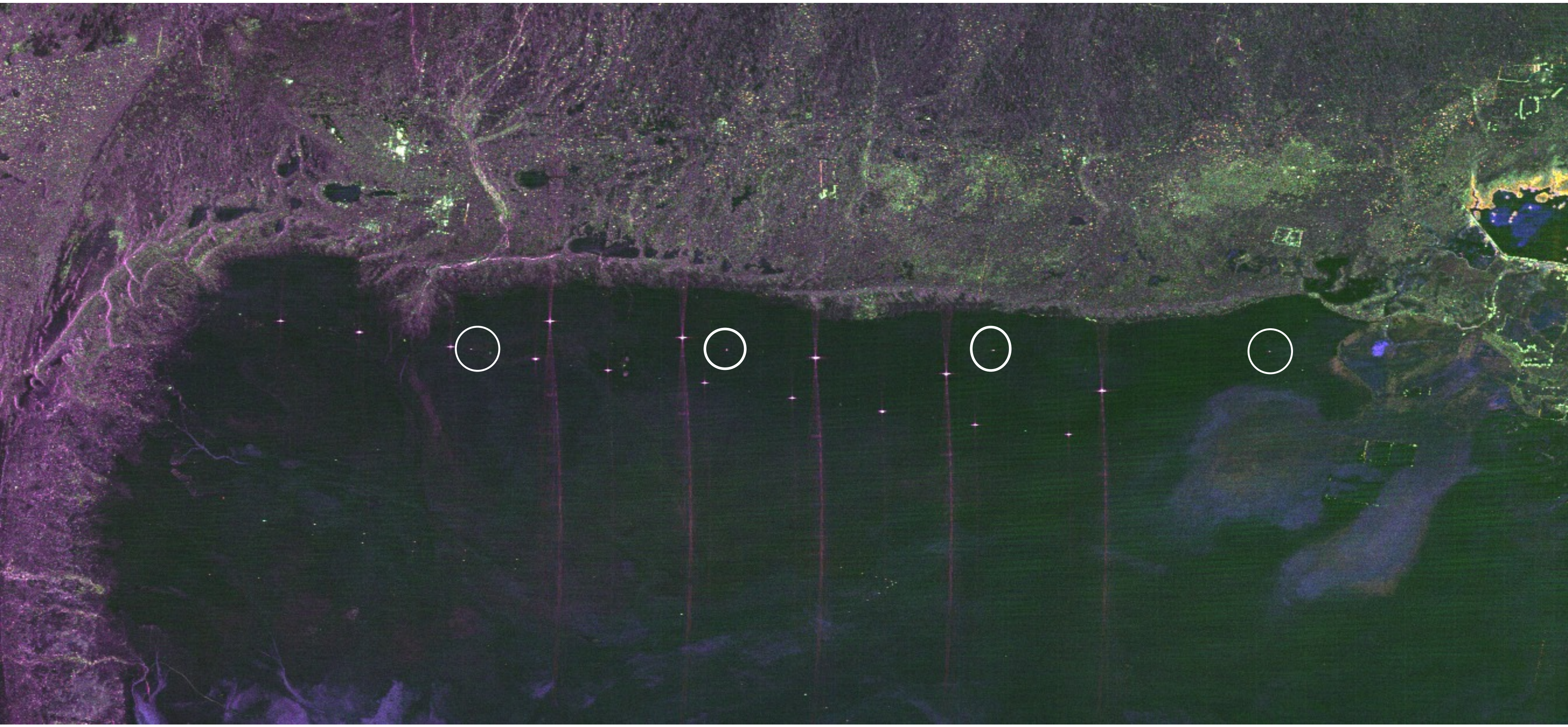

5   4.8 meter corners – all with 350 degree azimuth heading

23   2.4 meter corners – 10 with 350 heading, 13 with 170 heading

10   0.7 meter corners – 4 with 350 heading, 6 with 90 heading

0.7 Meter Trihedral Corner Reflector for Ka-band

4 at 350 heading (installed Dec, 2015), 6 at 90 heading (installed June, 2018)

2.4-meter Trihedral Corner Reflector for L-band

10 at 350 heading, 13 at 170 heading

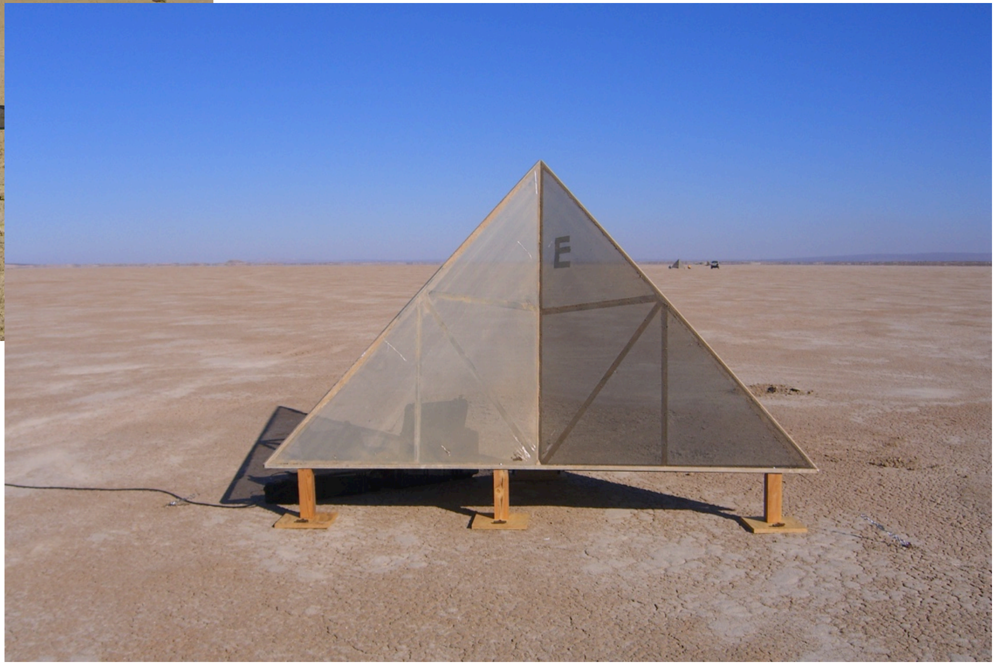

2.4-meter Trihedral Corner Reflector for L-band

CR#01, #02, #03, #04, #12 resurveyed Nov 1st, 2018

CR#17 repositioned Nov 7th, 2018

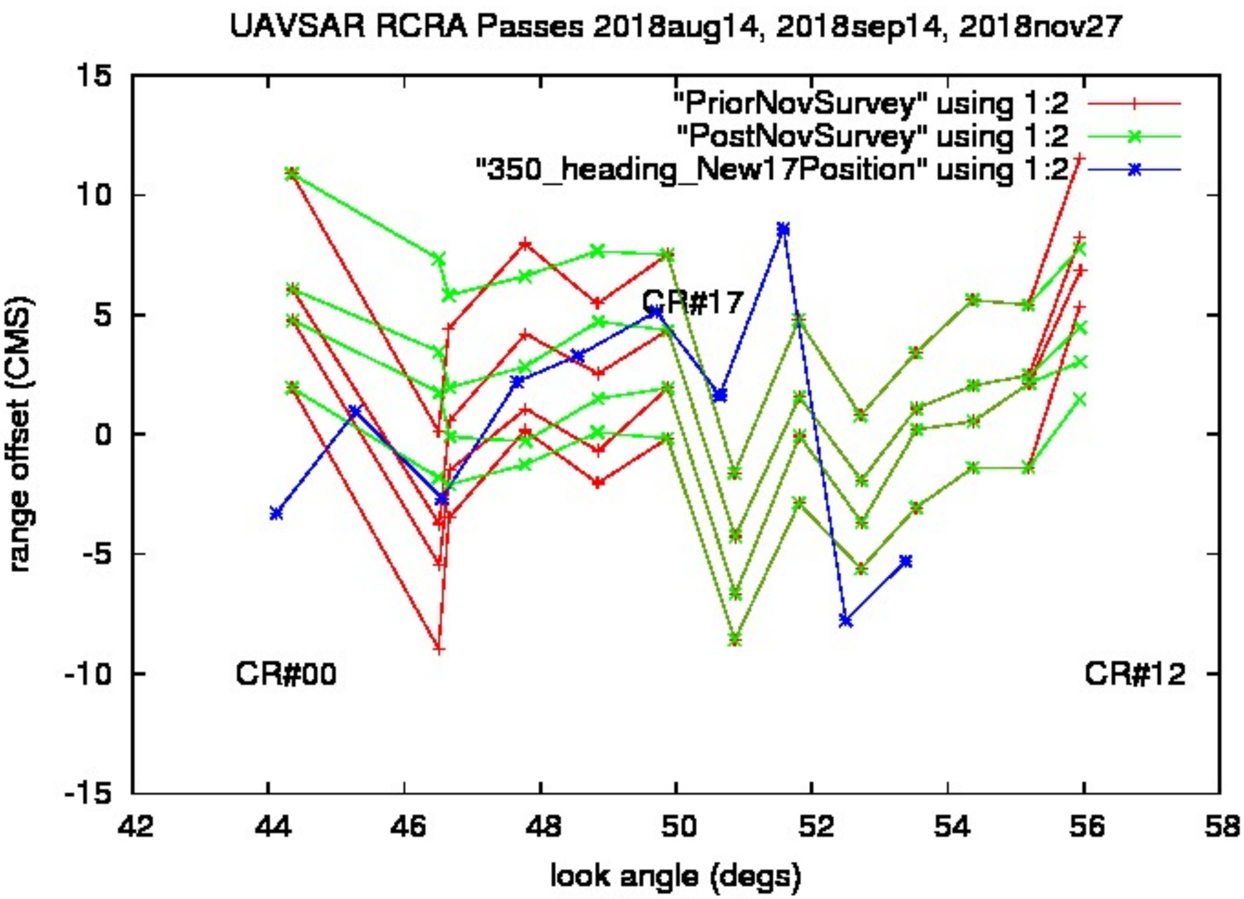

CR#17 moved
16 meters West
6 meters North

Need to resurvey CR#00, CR#06, CR#07, CR#08 then all the 170 heading CRs should then have a range accuracy of better than 1.2 CMS RMS.

https://uavsar.jpl.nasa.gov/cgi-bin/calibration.pl

4.8 meter Trihedral for P-band (and L-band)

5 at 350 heading (installed May, 2012)

Single Antenna Polarimetric Active Radar Calibrator

Single Antenna PARC

- Receives/Transmits through a single antenna with a dual-polarized horn.
- Uses an orthomode transducer (OMT) that provides 60 dB isolation between dual-pole transmitting and receiving polarizations.
- Reduces signal leakage within the antenna with passive leakage cancelation circuitry.
- Achieves an active gain by monitoring a reference signal generated by temperature regulated voltage controlled crystal oscillator (VCXO).
- Has an equal magnitude scattering matrix response due to 45 degree rotation in plane perpendicular to direction of incidence.

$$S_{PARC} = \begin{pmatrix} S_{HH} & S_{HV} \\ S_{VH} & S_{VV} \end{pmatrix} = \begin{pmatrix} 1 & 1 \\ -1 & -1 \end{pmatrix} \qquad S_{Trihedral} = \sqrt{\sigma_{cr}} \begin{pmatrix} 1 & 0 \\ 0 & 1 \end{pmatrix}$$

$$\emptyset_{HH-VV} = \emptyset_{HV-VH} = \pi \qquad \emptyset_{HH-VV} = 0$$

$$\emptyset_{HH-HV} = \emptyset_{VH-VV} = 0$$

Sarabandi, K., Oh, Y., Ulaby, F., "Performance Characterization of Polarimetric Active Radar Calibrators and a New Single Antenna Design," in IEEE Transactions On Antennas and Propagation, Vol. 40, No. 10, October 1992.

- Can evaluate cross-pol response, which cannot be estimated by passive trihedral targets.
- Provides direct computation of the cross-pol channel imbalance.

Single Antenna PARC

- High signal-to-clutter ratio.
  - To reduce calibration errors.
  - Has a configurable RCS value from 40 dBsm to 55 dBsm.
    - 55 dBsm @ L-band ~ to a 8.1 meter Trihedral CR with a 11.5 meter leading edge
- Can be deployed for remote operation.
  - Has a self contained on-board processor, receiver and digitizer.
  - Contains communication equipment for data storage and download.
  - Is solar powered, with rechargeable 24 Volt, 100 Ah Lithium Battery.
  - Has thermoelectric cooling to extend its application to high temp environment.
- Mature and sophisticated tools for remote programmability
  - WEB based scheduling for satellite passes.
  - SMS (cell phone) interface for instantaneous elevation and RCS settings.
  - Hand-held controller which accommodates a SAR indicator light.
  - New mobile device app available.
  - Hosts self diagnostics.
  - Logs engineering data to WEB.

NISAR and UAVSAR Clutter Statistics

Assuming -5 dBsm clutter background*

NISAR/UAVSAR clutter characteristics												
		NISAR										UAVSAR
Mode #		10	20	30	40	50	60	54	43	63	56	
Range Bandwidth	MHz	25	80	5	25	45	45	45	25	45	45	80
Ground Range Res. (n)	m	13.44	3.35	53.77	13.44	6.72	6.72	6.72	13.44	6.72	6.72	
Ground Range Res. (f)	m	10.21	2.84	40.86	10.21	5.11	5.11	5.11	10.21	5.11	5.11	1.67
Azimuth Resolution	m	6.05	6.05	6.05	6.05	6.05	6.05	6.05	6.05	6.05	6.05	0.8
Ground pixel size (n)	m^2	81.3	20.3	325.3	81.3	40.7	40.7	40.7	81.3	40.7	40.7	
Ground pixel size (f)	m^2	61.8	17.2	247.2	61.8	30.9	30.9	30.9	61.8	30.9	30.9	1.34
Ave. Clutter RCS (n)	dBsm	14.1	8.1	20.1	14.1	11.1	11.1	11.1	14.1	11.1	11.1	
Ave. Clutter RCS (f)	dBsm	12.9	7.4	18.9	12.9	9.9	9.9	9.9	12.9	9.9	9.9	-3.7

*Rosamond Dry Lake Bed clutter background is < -30 dBsm

NISAR and UAVSAR Clutter Statistics

UAVSAR/ NISAR power characteristics		
	UAVSAR	NISAR
Peak Transmit Power	3.1 kW	1.2 kW
Antenna Gain	18.9 dBi	34.8 dBi
Operation Altitude	12.5 Km	600 Km
Look Angle (deg)	15-60	30-41
PARC Received Power	-19dBm	-41dBm
PARC active gain	37 dB	52 dB
PARC transmit power	18 dBm	11 dBm

PARC SPECS		
	UAVSAR	NISAR
Frequency Range	1217.5 -1317.5MHz	
Bandwidth	100 MHz	
Antenna Gain	16.5 dBi	
Active Gain	37dB	52dB
RCS	40 dBsm	55 dBsm
Worse Case Signal to Clutter ratio	43.7 dB	34.9 dB
Max power	<20dBm (0.1 Watt)	

First Installed November 1, 2018

And UAVSAR Flight and Data Collect November 7, 2018

Compute PARC RCS from Standard Calibration

Backscatter SAR assumes reciprocity such that Shv = Svh

results in calibration coefficients as such:

$$\Sigma_{HH} = \frac{1}{A} = \frac{\sqrt{\sigma_{cr}}}{\sqrt{RCS(HH)_{observed}}}$$

$$\Sigma_{HV} = \frac{1}{Afg} = \sqrt{\Sigma_{HH}}\sqrt{\Sigma_{VV}}\ \frac{\left(\sqrt{\langle S_{VH}\ S_{VH}^{*}\rangle}\right)^{\frac{1}{2}}}{\left(\sqrt{\langle S_{HV}\ S_{HV}^{*}\rangle}\right)^{\frac{1}{2}}}$$

$$\Sigma_{VH} = \frac{g}{Af} = \sqrt{\Sigma_{HH}}\sqrt{\Sigma_{VV}}\ \frac{\left(\sqrt{\langle S_{HV}\ S_{HV}^{*}\rangle}\right)^{\frac{1}{2}}}{\left(\sqrt{\langle S_{VH}\ S_{VH}^{*}\rangle}\right)^{\frac{1}{2}}}$$

$$\Sigma_{VV} = \frac{1}{Af^2} = \frac{\sqrt{\sigma_{cr}}}{\sqrt{RCS(VV)_{observed}}}$$

$where\ A^2 = \frac{\langle S_{HH}\ S_{HH}^{*}\rangle}{\sigma_{cr}}\ and\ f^{\,4} = \frac{\langle S_{VV}\ S_{VV}^{*}\rangle}{\langle S_{HH} S_{HH}^{*}\rangle}$ are computed at the CR

$g^4 = \frac{\langle S_{HV}\ S_{HV}^{*}\rangle}{\langle S_{VH} S_{VH}^{*}\rangle}$ is computed within the image

PARC and CR RCS Comparison

Five 350 Degree Heading Data Lines over RCRA
with cross-pol channel imbalance = 1.2912

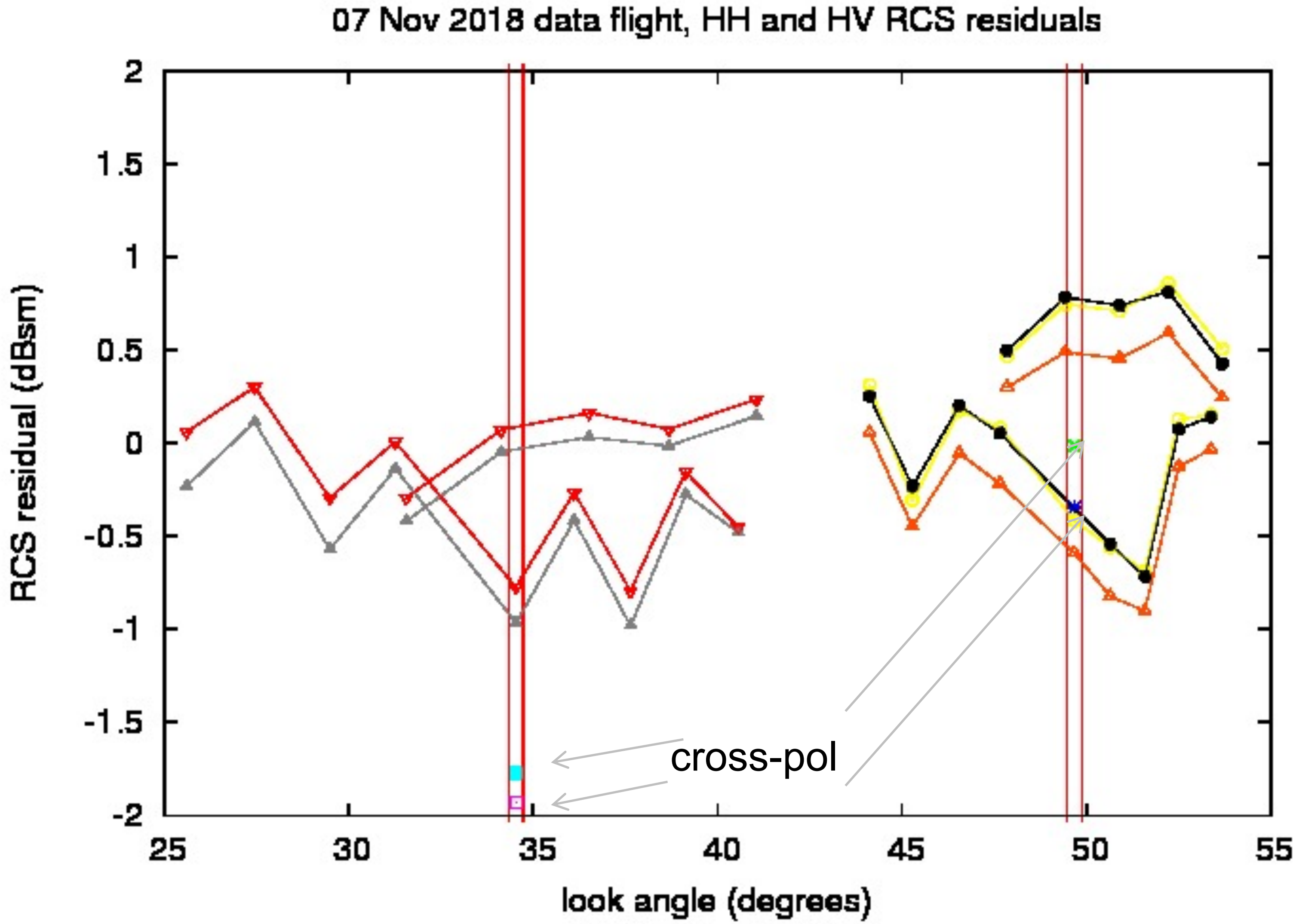

PARC and CR RCS Comparison

Five 350 Degree Heading Data Lines over RCRA with cross-pol channel imbalance = 1.2912

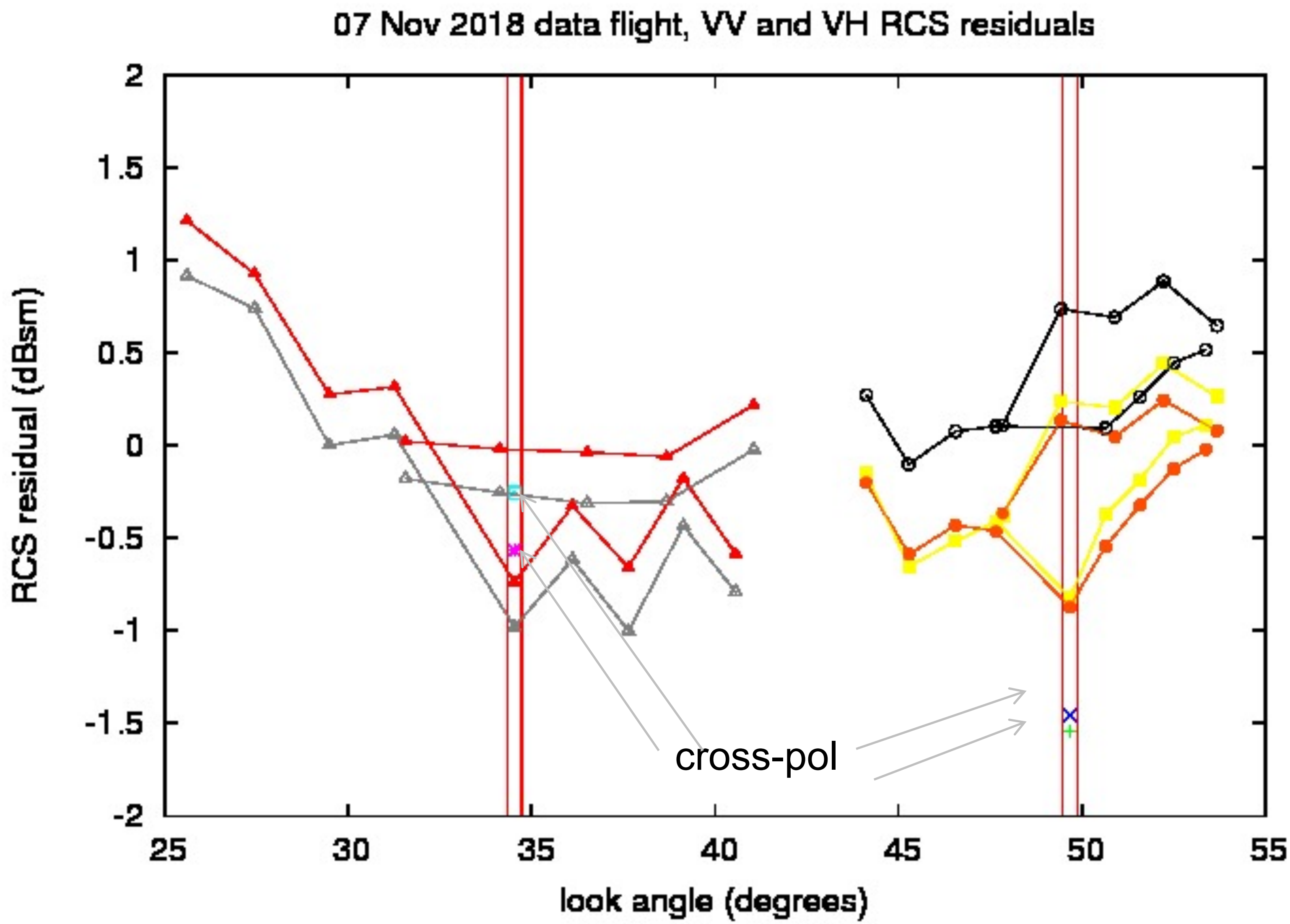

PARC Phase Comparison
Five 350 Degree Heading Data Lines over RCRA

For PARC, recall that: $\emptyset_{HH-VV} = \emptyset_{HV-VH} = \pi$

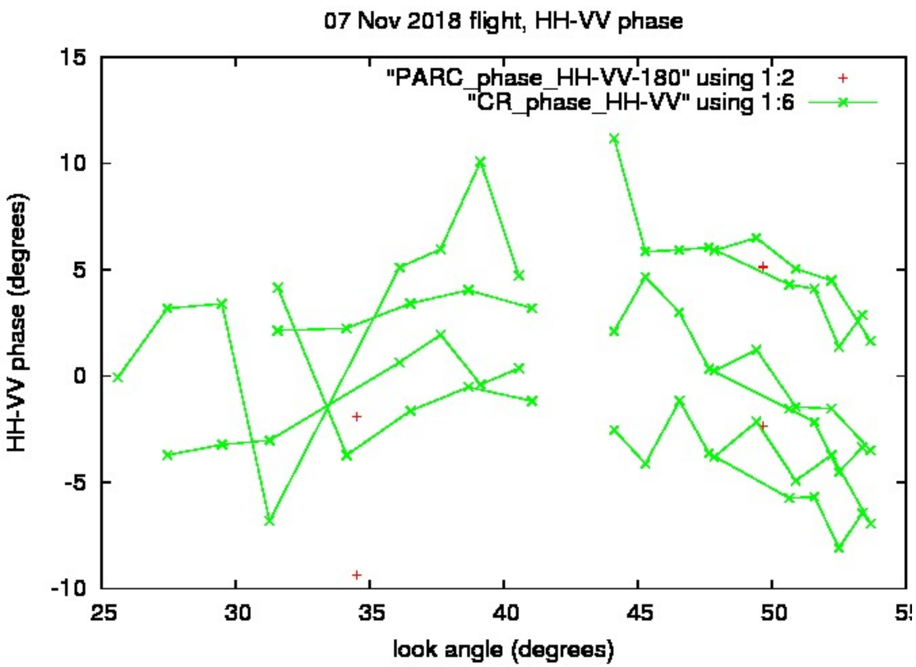

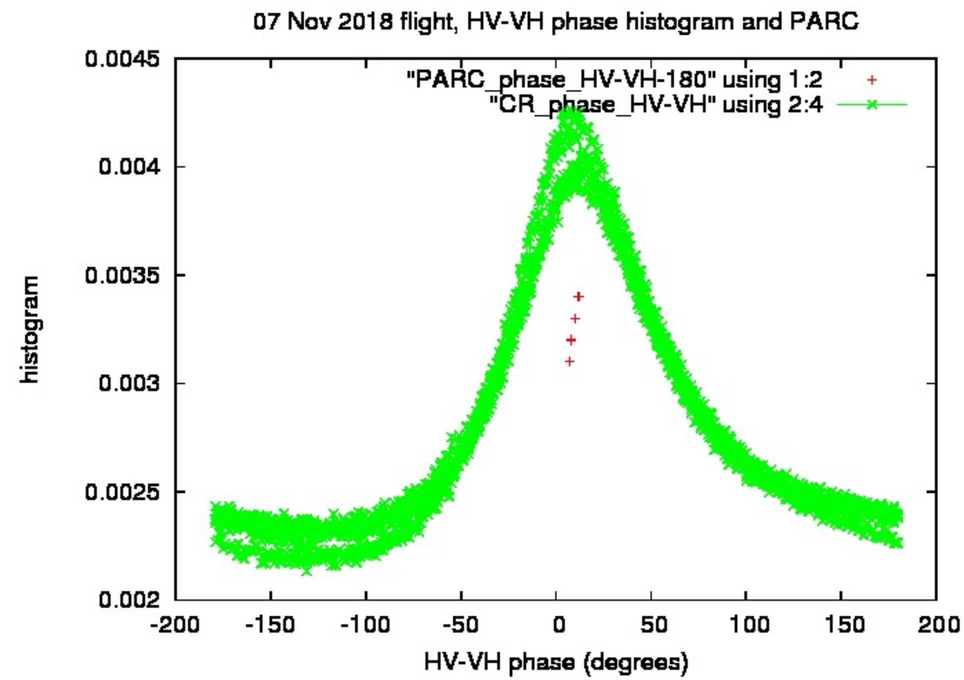

$\emptyset_{HH-VV}$ is computed at the CR

$\arg(\langle S_{HV}, S_{VH}^{*}\rangle)$ is computed within the image

Using the PARC for Calibration

of the Cross-Pol Channel Imbalance

$$\Sigma_{HH} = \frac{1}{A} = \frac{\sqrt{\sigma_{cr}}}{\sqrt{RCS(HH)_{observed}}}$$

$$\Sigma_{HV} = \frac{1}{Afg} = \sqrt{\Sigma_{HH}}\sqrt{\Sigma_{VV}}\;\frac{\left(\sqrt{\langle S_{VH}\, S_{VH}^*\rangle}\right)^{\frac{1}{2}}}{\left(\sqrt{\langle S_{HV}\, S_{HV}^*\rangle}\right)^{\frac{1}{2}}}$$

$$\Sigma_{VH} = \frac{g}{Af} = \sqrt{\Sigma_{HH}}\sqrt{\Sigma_{VV}}\;\frac{\left(\sqrt{\langle S_{HV}\, S_{HV}^*\rangle}\right)^{\frac{1}{2}}}{\left(\sqrt{\langle S_{VH}\, S_{VH}^*\rangle}\right)^{\frac{1}{2}}}$$

$$\Sigma_{VV} = \frac{1}{Af^2} = \frac{\sqrt{\sigma_{cr}}}{\sqrt{RCS(VV)_{observed}}}$$

$where\ A^2 = \frac{\langle S_{HH}\ S_{HH}^*\rangle}{\sigma_{cr}}\ and\ f^{\,4} = \frac{\langle S_{VV}\, S_{VV}^*\rangle}{\langle S_{HH} S_{HH}^*\rangle}$ are computed at the CR

$\underline{but\ now}\ g^4 = \frac{\langle S_{HV}\, S_{HV}^*\rangle}{\langle S_{VH} S_{VH}^*\rangle}$ is computed by the PARC at the CR

Using the PARC for Calibration

of the Cross-Pol Channel Imbalance

	from image	from PARC	Look Ang.
Rosamd_35012_000	1.3414	1.4100	49.7
Rosamd_35017_001	1.3085	1.1938	34.5
Rosamd_35012_013	1.3404	no value	
Rosamd_35017_014	1.2503	1.1828	34.5
Rosamd_35012_017	1.2154	1.3766	49.7
Average	1.2912	1.2908	

Using the PARC for Calibration

Computation of Cross-Pol calibration coefficients from PARC

$$\Sigma_{HH} = \frac{\sqrt{\sigma_{cr}}}{\sqrt{RCS(HH)_{observed}}}$$

$$\Sigma_{HV} = \frac{Equivalent\_PARC\_RCS\_Setting}{\sqrt{RCS(HV)_{observed}}}$$

$$\Sigma_{VH} = \frac{Equivalent\_PARC\_RCS\_Setting}{\sqrt{RCS(VH)_{observed}}}$$

$$\Sigma_{VV} = \frac{\sqrt{\sigma_{cr}}}{\sqrt{RCS(VV)_{observed}}}$$

$$where\ co-channel\ imbalance\ \ f^4 = \frac{\langle S_{VV}\, S_{VV}^{*}\rangle}{\langle S_{HH} S_{HH}^{*}\rangle} = \frac{\Sigma_{HH}^2}{\Sigma_{VV}^2}$$

$$and\ cross-channel\ imbalance\ g^4 = \frac{\langle S_{HV}\, S_{HV}^{*}\rangle}{\langle S_{VH} S_{VH}^{*}\rangle} = \frac{\Sigma_{VH}^2}{\Sigma_{HV}^2}$$

PARC and CR RCS Comparison

Five 350 Degree Heading Data Lines over RCRA with effective cross-pol channel imbalance = 1.2850 (was 1.2912)

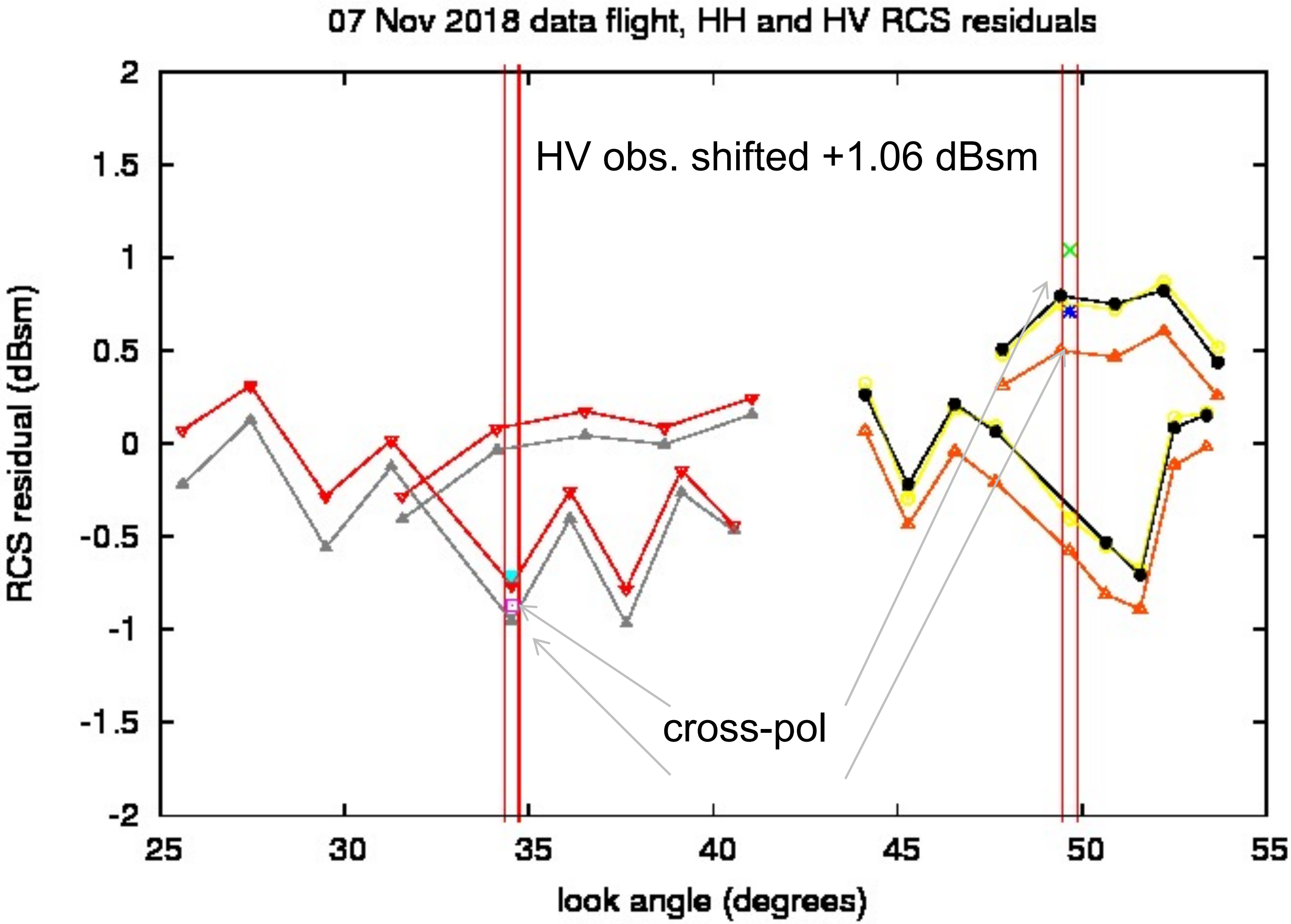

PARC and CR RCS Comparison

Five 350 Degree Heading Data Lines over RCRA
with effective cross-pol channel imbalance = 1.2850 (was 1.2912)

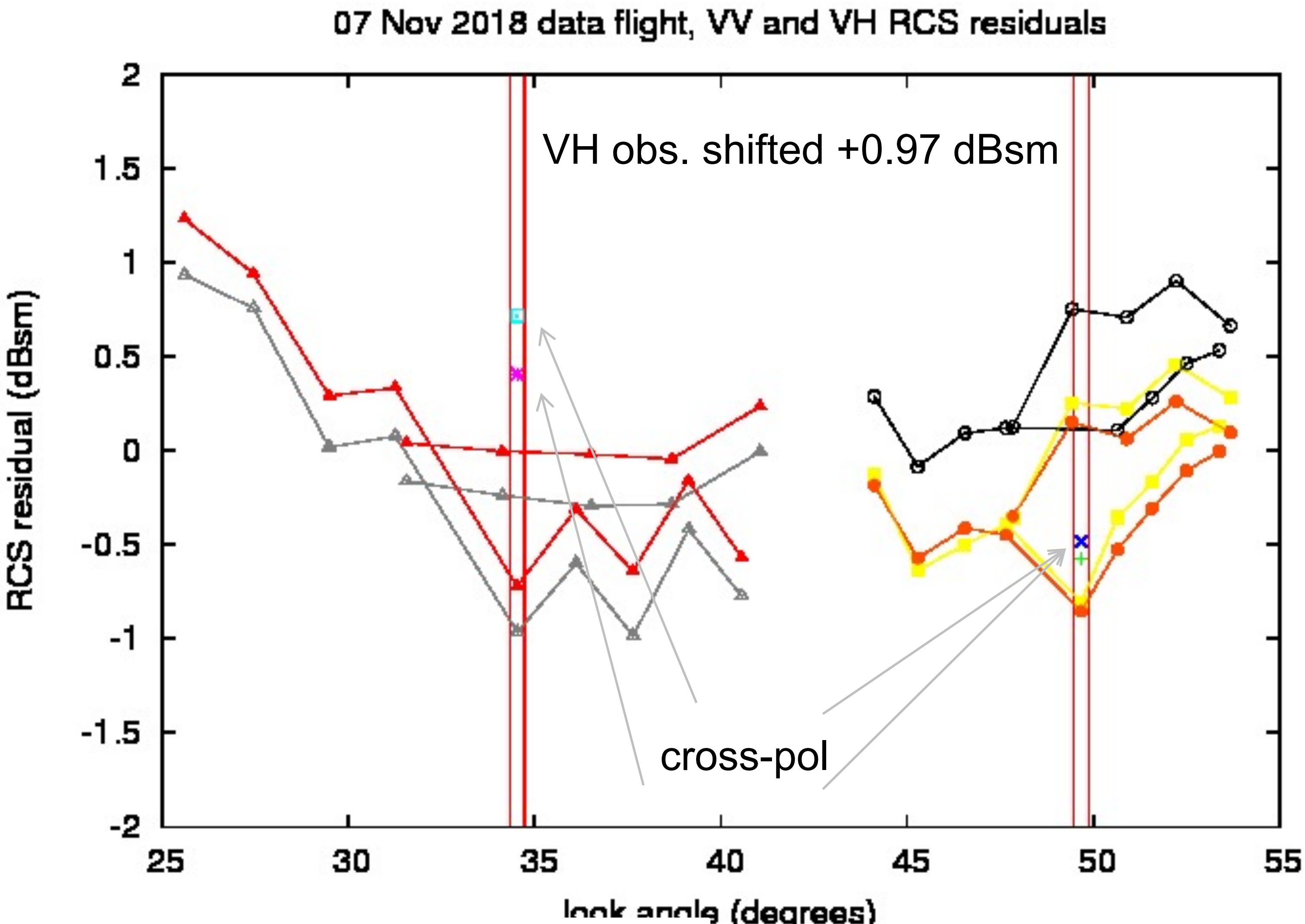

Observing the Platform Antenna Pattern

Account for one-way path loss

$$PathLoss_{dB} = 20\ log_{10}\ Range$$

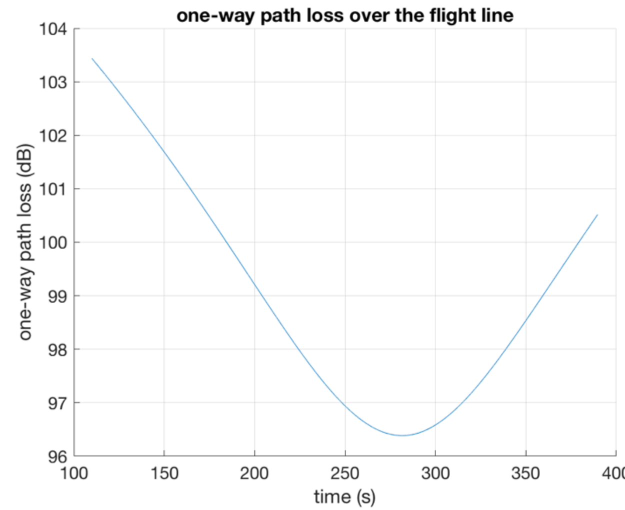

Account for PARC antenna pattern of 45 degree rotated horn antenna

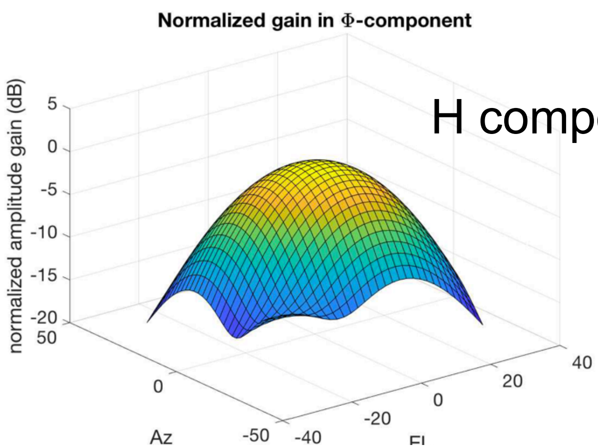

H component

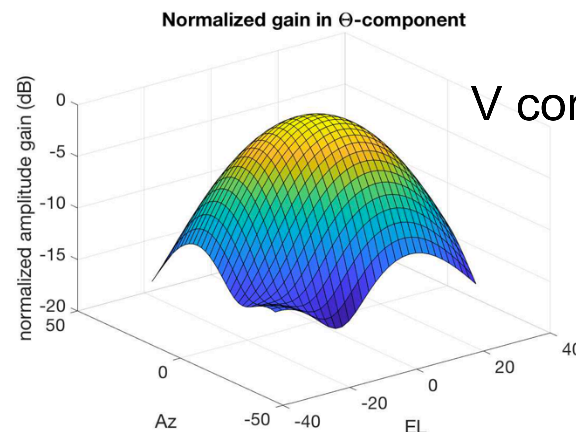

V component

$$ParcAntGain_{H,dB} = 13.5 + 20\ log_{10}\ \left|G_{\phi}(El, Az)\right|$$
$$ParcAntGain_{V,dB} = 13.5 + 20\ log_{10}\ \left|G_{\theta}(El, Az)\right|$$

Observing the Platform Antenna Pattern

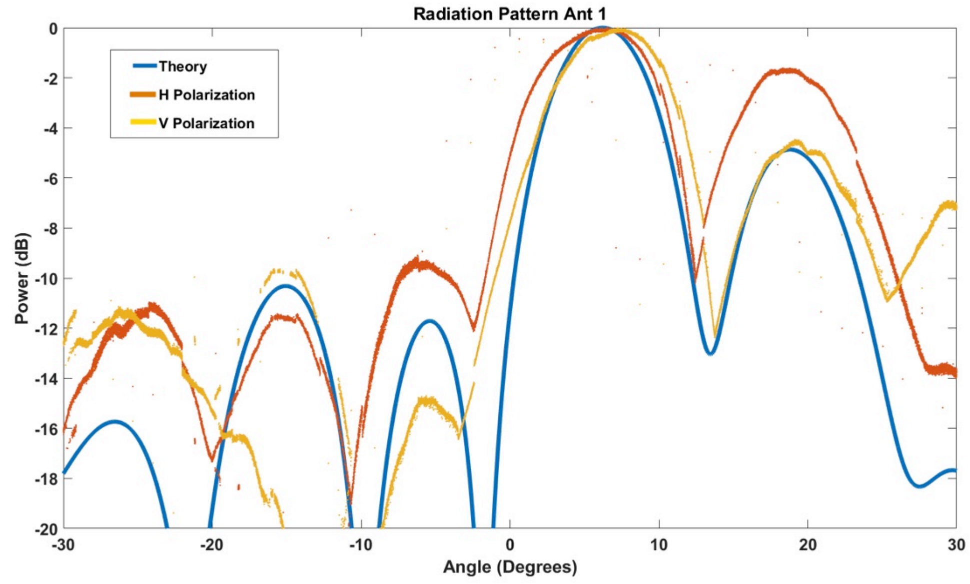

Nov 7th data flight included passes with two different antenna tables, BT101 and Ant 1.

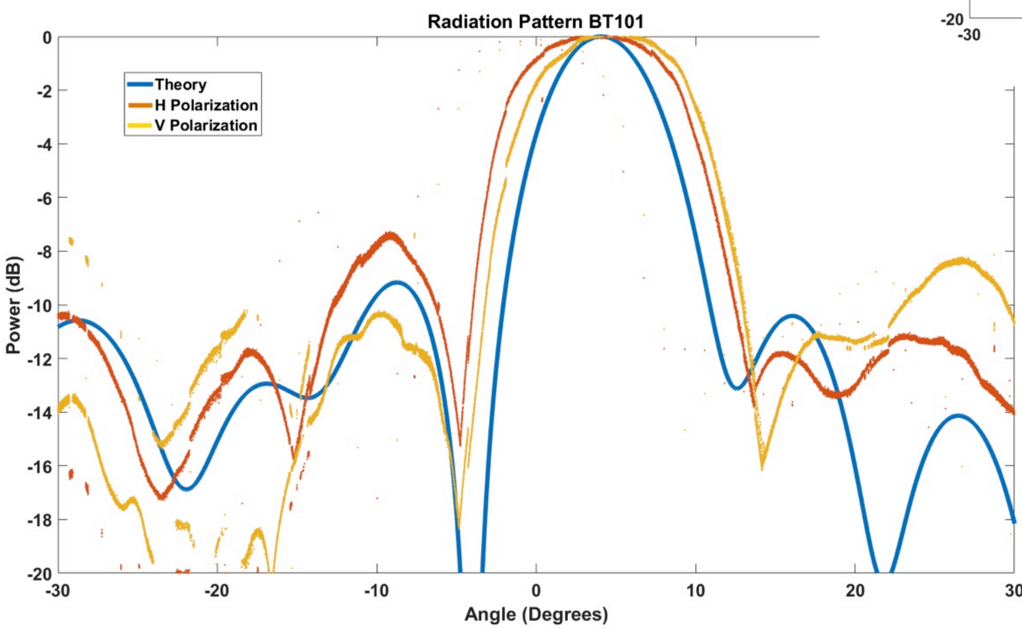

The predicted model computed from Beam Table Generator code using ~10Y old TR module measurement responses.

Phase Tracking the Peak Magnitude of Range Compressed Data Provides Relative Range Error of Platform

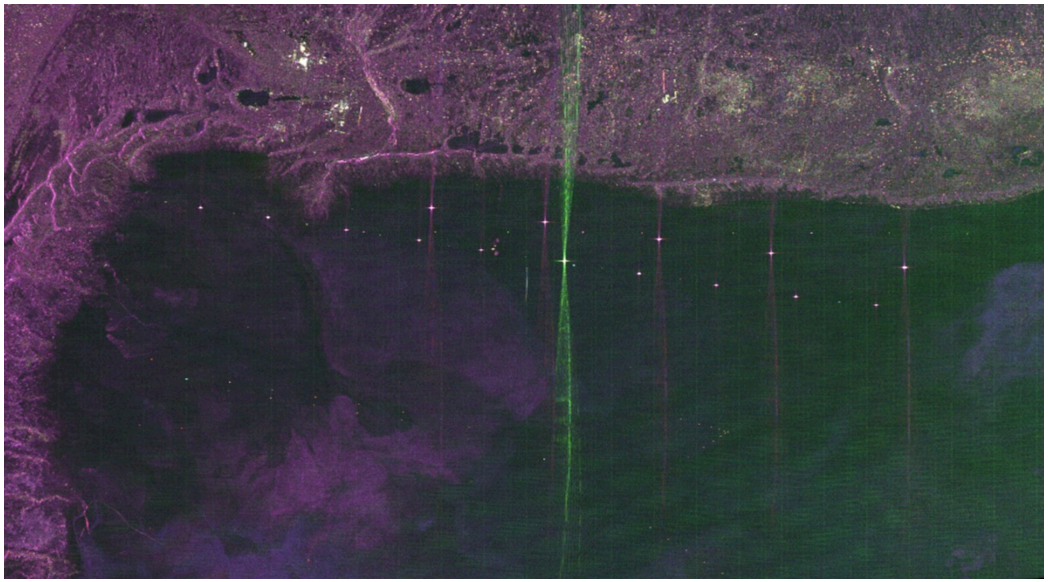

$$\delta r = f(corner, platform, trop)$$

$$\varphi = \arg\left(S_{\max} \times e^{\frac{4\pi i \delta r}{\lambda}}\right)$$

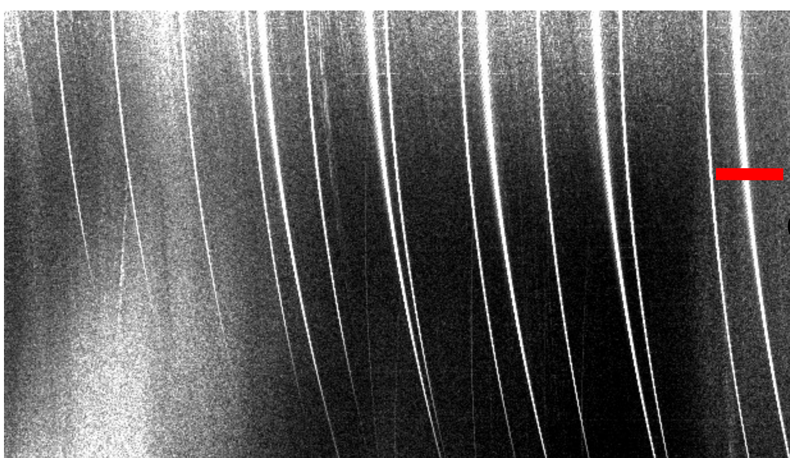

oversample

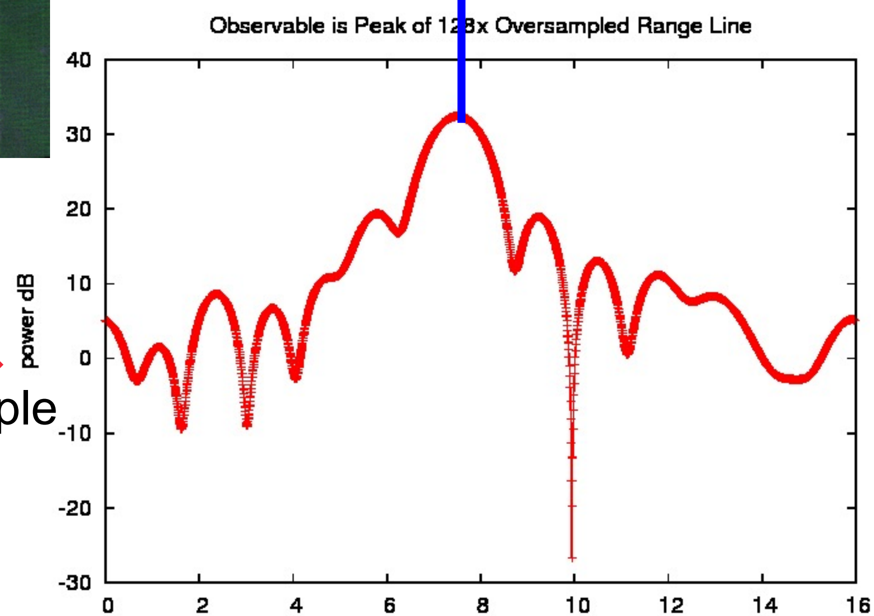

Phase Tracking the PARC

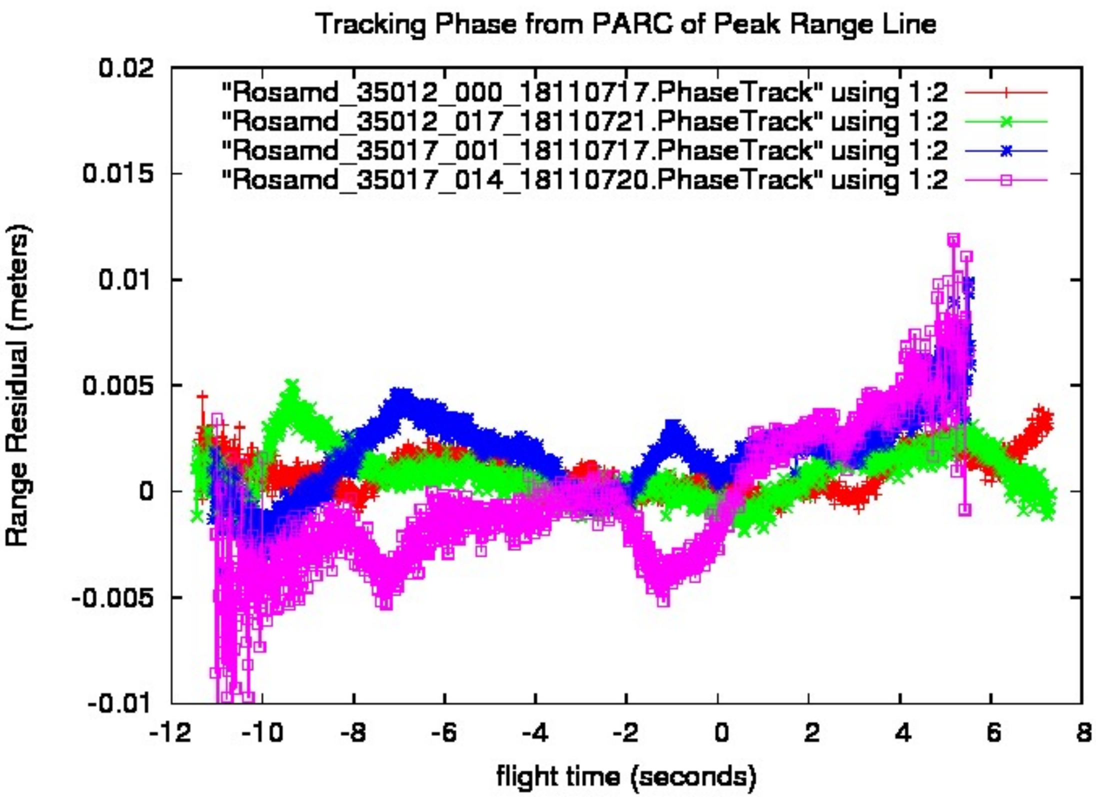

Preliminary computations show that the phase center of the PARC is 16.8 CMS below the face of the PARC with a 26.6 nsec time delay.

Data Line	PARC Setting	Look Angle	Range Error RMS
35012_000 (mid)	45 dBsm	49.7 degrees	1.2 mm
35012_017 (mid)	45 dBsm	49.7 degrees	1.4 mm
35017_001 (near)	45 dBsm	34.5 degrees	2.5 mm
35017_014 (near)	40 dBsm	34.5 degrees	3.2 mm

Summary

- University of Michigan has delivered to UAVSAR-- a JPL/NASA institutional instrument-- a Single Antenna Polarimetric Active Radar Calibrator.
  - Second PARC to be delivered in 2019.
- First data acquired from the PARC was from UAVSAR on November 7th, 2018
- Good Co-Pol and RCS agreement with Trihedral Corners at RCRA.
  - Possible ~ 1dBsm look-angle dependent Cross-Pol (very preliminary).
- Good HH-VV phase agreement with CRs.
- Very good HV-VH phase agreement with background.
- Amplitude data from PARC ground acquisitions agrees with predicted UAVSAR transmit antenna pattern.
  - Goal is to prepare an optimum antenna table for existing L-band Antenna.
- Phase tracking the PARC return at 45 dBsm shows several mm of platform (UAVSAR) range error over 20 seconds.
  - Expectation is to increase PARC RCS to 55 dBsm to acquire 40 seconds (at least 2 patches) of L-band data to aid in tuning the platform metrology stochastic modeling.
- Need to investigate effect of ~27 nsec PARC time delay and the effect on SAR focusing and RCS.

Jet Propulsion Laboratory
California Institute of Technology

jpl.nasa.gov